

Probing the ΔNN component of ${}^3\text{He}$

G. M. Huber,^{1,*} G. J. Lolos,¹ E. J. Brash,¹ S. Dumalski,¹ F. Farzanpay,¹ M. Iurescu,¹ Z. Papandreou,¹ A. Shinozaki,^{1,3} A. Weinerman,¹ T. Emura,² H. Hirosawa,² K. Niwa,² H. Yamashita,² K. Maeda,³ T. Terasawa,³ H. Yamazaki,³ S. Endo,⁴ K. Miyamoto,⁴ Y. Sumi,^{4,†} G. Garino,⁵ K. Maruyama,⁵ A. Leone,⁶ R. Perrino,⁶ T. Maki,⁷ A. Sasaki,⁸ and Y. Wada⁹

(The TAGX Collaboration)

¹Department of Physics, University of Regina, Regina, Saskatchewan, Canada S4S 0A2

²Department of Applied Physics, Tokyo University of Agriculture and Technology, Koganei, Tokyo 184, Japan

³Department of Physics, Tohoku University, Sendai 980, Japan

⁴Department of Physics, Hiroshima University, Higashi-Hiroshima 724, Japan

⁵Institute for Nuclear Study, University of Tokyo, Tanashi, Tokyo 188, Japan

⁶INFN-Sezione di Lecce, I-73100 Lecce, Italy

⁷University of Occupational and Environmental Health, Kitakyushu 807, Japan

⁸College of General Education, Akita University, Akita 010, Japan

⁹Meiji Pharmaceutical University, Kiyose, Tokyo 204, Japan

(Received 17 April 2000; published 13 September 2000)

The ${}^3\text{He}(\gamma, \pi^\pm p)$ reactions were measured simultaneously over a tagged photon energy range of $800 \leq E_\gamma \leq 1120$ MeV, well above the Δ resonance region. An analysis was performed to kinematically isolate Δ knockout events from conventional Δ photoproduction events, and a statistically significant excess of $\pi^+ p$ events was identified, consistent with Δ^{++} knockout. Two methods were used to estimate the ΔNN probability in the ${}^3\text{He}$ ground state corresponding to the observed knockout cross section. The first gave a lower probability limit of $1.5 \pm 0.6 \pm 0.5\%$; the second yielded an upper limit of about 2.6%.

PACS number(s): 27.10.+h, 14.20.Gk, 21.45.+v, 25.20.Lj

I. MOTIVATION

For the last 25 years, the question of whether Δ isobars are present in the nuclear ground state with any significant probability has been raised. Many theoretical calculations support this conjecture. For example, a detailed calculation by Anastasio *et al.* [1] for the deuteron, ${}^{16}\text{O}$, and infinite nuclear matter found that the Δ content could be as high as 7.5%, depending on the region of Fermi momentum probed and the potential used to describe the $NN \rightarrow \Delta N$ transition. Similarly, a NN and $\Delta\Delta$ coupled channel calculation with quark degrees of freedom at short range finds it necessary to include a 5–7% $\Delta\Delta$ content in the deuteron ground state to adequately describe the recent T_{20} results from Jefferson Laboratory, together with the deuteron magnetic moment and np scattering data [2]. It would indeed be surprising if nuclei had no Δ component, because of the strong one-pion-exchange tensor coupling to the $\Delta\Delta$ and $N\Delta$ channels. This is confirmed by the many models incorporating nuclear Δ content at the few percent level [3]. Nonetheless, experimental support for this concept remains elusive.

A fundamental limitation of all experimental searches for preexisting Δ 's in nuclei is that assumptions must be made in the effort to link some observed “ Δ component signal” to the corresponding wave function probability. Each experiment is sensitive to a particular range of Fermi momenta,

while the wave function probability is integrated over all possible momenta. Therefore, the extraction of the Δ configuration probability is model dependent, and it is not surprising that the experimental searches have sometimes yielded contradictory results. It is necessary to perform studies in as many complementary manners as possible, in order to obtain a quantitative understanding of this issue.

Emura *et al.* [4] estimated the ΔNN component of ${}^3\text{He}$ to be $< 2\%$, based on the asymmetry of $\pi^\pm p$ yields obtained with 380–700 MeV tagged photons. While cuts were placed to separate conventional quasifree $\gamma N \rightarrow \Delta$ production from any Δ knockout signal, contamination from non- Δ processes remained in the data sample, and so the result is not conclusive. Amelin *et al.* [5] identified Δ^{++} knockout from ${}^9\text{Be}$ by 1 GeV protons by detecting the recoil ${}^8\text{He}$ and estimated the ratio of the $\Delta^{++}{}^8\text{He}$ and $p{}^8\text{Li}$ spectroscopic factors to be $(6 \pm 3) \times 10^{-4}$. However, this method only probes the quasi-bound component of the recoil system, and a further correction would have to be attempted to yield a definitive result. Electroproduction measurements hold much promise, because the use of longitudinal virtual photons can provide an effective means of separating the Δ knockout and conventional production mechanisms, especially in a triple coincidence ($e, e' \pi^\pm p$) measurement. A Mainz experiment [6] performed a longitudinal/transverse (L/T) separation of the ${}^3\text{He}(e, e' \pi^\pm)$ cross section at $\omega = 370$ – 430 MeV, and observed an unexpectedly large L/T ratio. Because preexisting Δ 's can absorb either longitudinal or transverse virtual photons, while Δ electroproduction is a predominantly transverse process, this “might be taken as a possible hint for the existence of a preformed Δ .” Quantitative agreement with a microscopic model, including pole terms, final state rescattering

*Corresponding author: TEL: 306-585-4240, FAX: 306-585-5659, electronic address: huberg@uregina.ca

†Present address: Department of Clinical Radiology, Hiroshima International University, Kurose-cho, Hiroshima 724-0695, Japan.

tering, and produced and preformed Δ resonances, was unfortunately too poor to allow extraction of the Δ component probability.

Perhaps the most interesting result was obtained with 500 MeV pions at LAMPF [7,8]. The double-charge-exchange reaction ($\pi^+, \pi^- p$) can only occur in one step if there is a preexisting Δ^- in the nucleus, in which case the reaction will follow quasifree $\pi^+ \Delta^- \rightarrow \Delta^0 \rightarrow \pi^- p$ kinematics. Targets ranging from ${}^3\text{H}$ to ${}^{208}\text{Pb}$ were used, and by comparison to quasifree ($\pi^+, \pi^+ p$) scattering Δ probabilities from 0.5% to 3.1% were extracted. Unfortunately, measurements were performed at only one or two angle pairs per target, and the extracted Δ probability varied by a factor of 2 for the different angle pair measurements on ${}^{12}\text{C}$, for example. The method holds much promise, but a conclusive measurement requires a systematic study over a larger range of ejectile angles.

Here, we present the result of a recent study of the ΔNN component of ${}^3\text{He}$. This is an especially interesting nucleus for two reasons. First, a Faddeev method calculation by Streuve *et al.* [9], explicitly involving NNN and ΔNN channels in the coupled-channel momentum-space approach, predicts the ΔNN component of the ${}^3\text{He}$ wave function to be significant, about 2.4%. Second, any ΔNN component in ${}^3\text{He}$ must have unique symmetry properties, making its experimental identification much easier. Indeed, any Δ 's present in nuclei must be deeply off shell, and so their existence can only be inferred on the basis of their isospin and spin properties. Since the Δ has $I=3/2$, the other two nucleons are required to be in an $I=1$ state to yield $I=1/2$ for the ${}^3\text{He}$ ground state. Therefore, since the two nucleons are in an isospin symmetric state, the spin state must be the antisymmetric 1S_0 . This forces the Δ to be in an $L=2$ state with respect to the NN pair to give an overall $J=1/2$ for ${}^3\text{He}$, and results in a unique kinematical signature, enabling us to distinguish preexisting Δ knockout from conventional Δ production processes.

Furthermore, coupling the $I=3/2$ Δ with the $I=1$ NN state to yield $I=1/2$ for ${}^3\text{He}$ gives the following decomposition for any ΔNN state in ${}^3\text{He}$:

$$|\Delta NN_{3\text{He}}\rangle = \sqrt{\frac{1}{2}}|\Delta^{++}nn\rangle - \sqrt{\frac{1}{3}}|\Delta^+pn\rangle + \sqrt{\frac{1}{6}}|\Delta^0pp\rangle.$$

Thus, from isospin considerations alone, if we perform a π photoproduction experiment and identify $\pi^+ p$ from Δ^{++} decay, and $\pi^- p$ from Δ^0 decay, we anticipate a yield ratio

$$\frac{\pi^+ p}{\pi^- p} = 9$$

from Δ knockout. In addition, the $\gamma\Delta^{++}$ interaction is substantially stronger than the $\gamma\Delta^0$ interaction, because of the double charge of the Δ^{++} , and so this ratio is further enhanced. These facts led Lipkin and Lee [10] to conclude that, ‘‘therefore, if a strong π^+ signal and no π^- detected in the

kinematic region in which the Δ -knockout mechanism can be unambiguously identified, it is a clear indication of the presence of Δ in ${}^3\text{He}$.’’

II. EXPERIMENT

The experiment was performed at the 1.3 GeV electron synchrotron located at the Institute for Nuclear Study (INS) of the University of Tokyo, with tagged photons of energy between $E_\gamma=800$ and 1120 MeV. This photon range is advantageous as the maximum of the $\gamma N \rightarrow \Delta$ quasifree process occurs near $E_\gamma=350$ MeV, and so exclusive Δ photoproduction on a single nucleon is suppressed by nearly two orders of magnitude. The tagged photon beam was incident upon a liquid ${}^3\text{He}$ target, and $\pi^+ p$, $\pi^- p$ coincidences were obtained simultaneously with the TAGX large acceptance magnetic spectrometer, with approximately π sr solid angle. For more details on the TAGX system, the reader is referred to Ref. [11]. The data were obtained concurrently with the ${}^3\text{He}(\gamma, \pi^+ \pi^-)$ results published in Refs. [12,13]. Events consisting of two charged particle tracks, one on each side of the photon beamline, with a proton of momentum >300 MeV/c (as reconstructed at the center of the target), in coincidence with either a π^+ or a π^- of momentum >100 MeV/c, were accepted for further analysis. If more than one proton was intercepted by the TAGX spectrometer, the one with the smallest scattering angle was selected, as Monte Carlo simulations indicated that this choice was more likely to be the Δ -associated proton. Both $\pi^+ p$ and $\pi^- p$ coincidence data were analyzed in an identical manner, and physics-motivated criteria were placed on the data to isolate the unique kinematical signature associated with preexisting Δ knockout. These criteria are explained below.

Figure 1 shows the missing mass distribution obtained with the TAGX detector. At these energies, a significant portion of the photoabsorption cross section is due to $\pi\pi$ production, and events associated with the production of a sec-

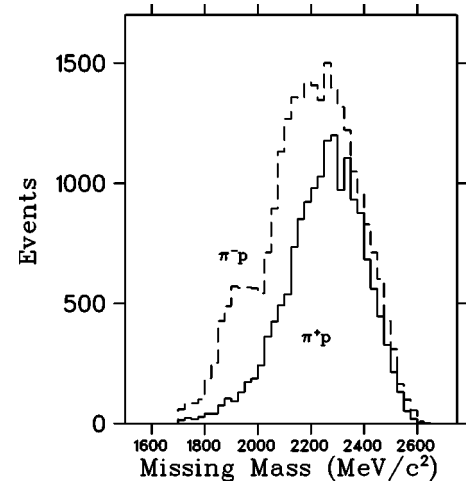


FIG. 1. Missing mass (MM) distributions for the ${}^3\text{He}(\gamma, \pi^\pm p)$ data obtained with TAGX with no ‘‘physics cuts’’ applied. $\pi^- p$ coincidences outnumber $\pi^+ p$ over the entire histogram. The condition $MM < 2m_N + m_\pi$ was subsequently applied to eliminate events associated with the production of a second, undetected, pion.

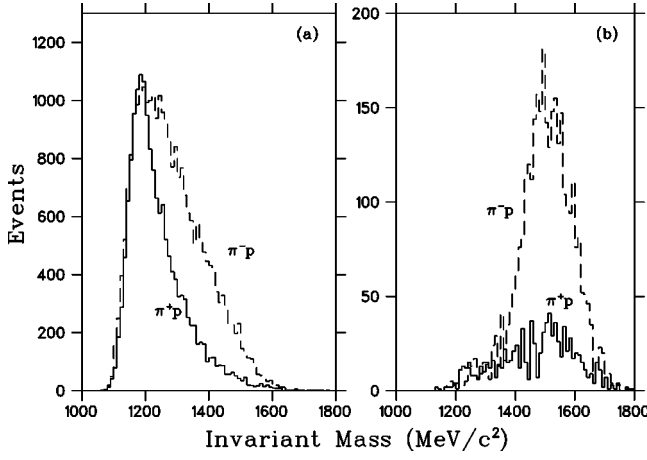


FIG. 2. Invariant mass (IM) distributions for the ${}^3\text{He}(\gamma, \pi^\pm p)$ data obtained with TAGX. Panel (a) has no physics cuts applied (as in Fig. 1), while panel (b) is subject to the requirement that $1700 < \text{MM} < 2020 \text{ MeV}/c^2$. The $\gamma n \rightarrow N^* \rightarrow p \pi^-$ channel is excluded from the remainder of the analysis by the placement of the additional requirement $\text{IM} \approx m_\Delta$.

ond (undetected) π were excluded by the requirement

$$\text{missing mass (MM)} < 2m_N + m_\pi. \quad (1)$$

It is well known that a $\pi^+ p$ pair forms a pure $I=3/2$ state, while a $\pi^- p$ pair forms a mixed $I=1/2, 3/2$ state. The effect of this asymmetry is shown clearly in Fig. 2. Panel (a) shows the invariant mass for all of the data, while panel (b) displays only those which passed the missing mass requirement of Eq. (1). It is observed that most of the $\pi^- p$ events in this panel are due to the production of the various N^* resonances. As the objective is to identify a subset of events which are due to Δ knockout, we exclude most of the remaining data with the requirement

$$\pi^\pm p \text{ invariant mass (IM)} \approx m_\Delta. \quad (2)$$

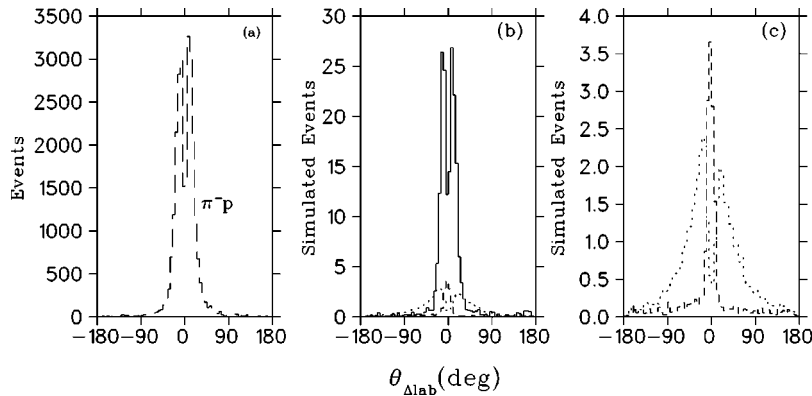


FIG. 3. Reconstructed Δ emission angle in the laboratory frame for the $\pi^- p$ channel. Panel (a) displays the data obtained by TAGX with no physics cuts applied. Panel (b) shows simulations of three different production mechanisms with arbitrary normalization. The solid line is two-pion production such as ${}^3\text{He}(\gamma, \pi^0 \Delta^0) pp$, and is removed from further analysis by the missing mass cut. Panel (c) shows expanded views of the quasifree Δ^0 photoproduction (dashed line) and Δ^0 knockout (dotted line) distributions. The two-nucleon mechanism is similar to the solid line. Quasifree production does not contribute to the $\pi^+ p$ channel, but is otherwise identical. Knocked-out Δ candidate events are preferentially selected via an additional requirement on $\theta_{\Delta \text{lab}}$. All simulations include the effect of the TAGX acceptance and resolution.

These two requirements leave a small number of $\pi^+ p$ events remaining, whose invariant mass is consistent with Δ decay and whose missing mass is too low to allow any undetected π to have been produced.

The $\Delta^{++} \rightarrow \pi^+ p$ channel can either be populated by pre-existing Δ^{++} knockout or by production processes involving more than one nucleon, such as $\gamma pp \rightarrow \Delta^{++} n$. The $\Delta^0 \rightarrow \pi^- p$ channel is ordinarily expected to be dominated by quasifree $\gamma n \rightarrow \Delta^0$ production, but this is suppressed by the choice of an incident photon energy well above the Δ region. The other two processes which can contribute to $\pi^- p$ production are preexisting Δ^0 knockout, which should occur at a much lower probability than Δ^{++} knockout, and multi-nucleon mechanisms such as $\gamma np \rightarrow \Delta^0 p$. Assuming that the isovector channel dominates photoabsorption at these energies, we anticipate that the multinucleon processes will contribute equally to both the $\pi^+ p$ and $\pi^- p$ channels, after accounting for the approximately 1.5 pn pairs in ${}^3\text{He}$.

To isolate the Δ knockout process from multinucleon Δ^{++} production, it is necessary to place an additional requirement upon the data. Since any preexisting Δ in ${}^3\text{He}$ must be in a $L=2$ state with respect to the NN pair prior to knockout, it corresponds to a high momentum component of the wave function. The angular distribution of the knocked-out Δ 's will be weighted by an additional q^4 factor compared to conventionally produced Δ 's from nucleons, resulting in a broad angular distribution. Our Monte Carlo simulations confirm that all non-knockout mechanisms produce Δ 's with forward-peaked angular distributions, while Δ 's from the knockout process are distributed broadly in angle (Fig. 3). This leads to the third requirement

$$|\theta_{\Delta \text{lab}}| > \theta_{\min}, \quad (3)$$

where θ_{\min} is sufficiently large to discriminate against the quasifree and two nucleon mechanisms.

The insensitivity of the result to the actual cuts employed is demonstrated in Fig. 4, in which two cuts are cyclically held constant and the third varied. In the case of θ_{IM} , a cut

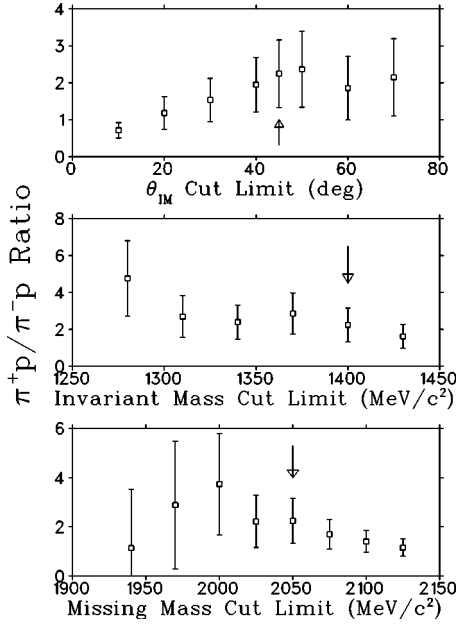


FIG. 4. Observed π^+p/π^-p ratio after two cuts are cyclically held constant and the third varied. The conditions held constant were $|\theta_{\text{IM}}| > 45^\circ$, $1070 < \text{IM} < 1400 \text{ MeV}/c^2$, and $1700 < \text{MM} < 2050 \text{ MeV}/c^2$. These values are denoted by the arrows on the various plots.

only on small angles does not adequately remove events from the quasifree peak, but background contributions are effectively suppressed when events with $|\theta_{\text{IM}}| > 40^\circ$ are removed, leading to a nearly constant ratio. In the case of the invariant mass cut, a narrow cut around the Δ peak results in a large excess of π^+p events, but at the expense of poor statistics. A broader cut results in a diluted, but more stable ratio. Finally, in the case of the missing mass, a cut to exclude only the highest MM events allows in a 2π back-

TABLE I. The two different sets of conditions employed upon the data and the number of events passing each.

	Cut values	π^+p events	π^-p events
	$1700 < \text{MM} < 2025 \text{ MeV}/c^2$		
Narrow	$1070 < \text{IM} < 1370 \text{ MeV}/c^2$ $ \theta_{\text{IM}} > 50^\circ$	38.2 ± 10.0	9.4 ± 17.2
	$1700 < \text{MM} < 2050 \text{ MeV}/c^2$		
Wide	$1070 < \text{IM} < 1400 \text{ MeV}/c^2$ $ \theta_{\text{IM}} > 45^\circ$	72.1 ± 14.5	32.1 ± 22.8

ground, which dilutes the ratio. In the end, two different sets of cuts were employed, to allow some estimate of the systematic error in the final result. These are summarized in Table I. While the data sample initially contained more π^-p than π^+p events ($25\,411 \pm 390$ versus $15\,733 \pm 295$), the application of conditions (1), (2), and (3) leads to a net excess of remaining π^+p events, compared to π^-p events.

To see whether these π^+p events have the kinematical signature appropriate to Δ knockout, they were compared to Monte Carlo simulations which take into account the TAGX resolution and acceptance and the effect of the applied conditions (1), (2), and (3). The modeled processes were the following.

(1) Quasifree $\gamma n \rightarrow \Delta^0$ production. The spectral function of Schiavilla, Pandharipande, and Wiringa [14] is assumed for the struck neutron and the Breit-Wigner distribution for the Δ . This quasifree process does not contribute to π^+p production.

(2) Δ production via two interacting nucleons, $\gamma NN \rightarrow \Delta N$, with the third nucleon being a spectator. The same spectral function as above is assumed.

(3) Quasifree $\gamma N \rightarrow \Delta \pi$, where the detected π^\pm may or may not originate from the Δ . Because of conditions (1) and

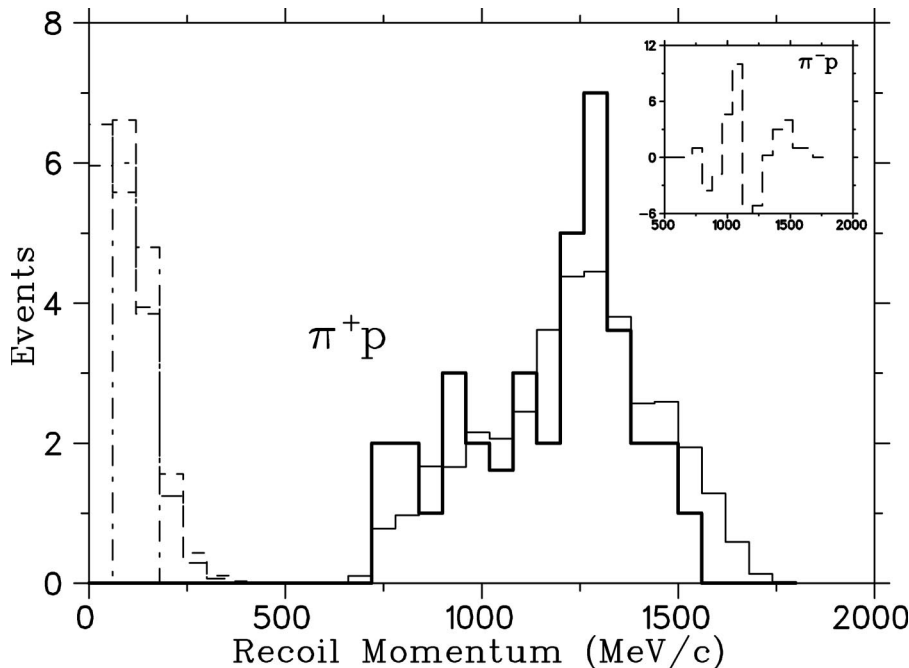


FIG. 5. Missing momentum after application of ‘‘narrow’’ conditions (1), (2), and (3). The dark line is the π^+p data, while the light line is the ΔNN phase-space simulation under the same conditions. The various dashed distributions on the left side of the plot are all of the other simulations, as described in the text. The inset shows the corresponding π^-p data, which are randomly distributed and carry little statistical significance. The negative events are due to the empty target data subtraction.

(2), this reaction is expected to be excluded from the data sample, but the simulation was included in the analysis, to ensure that the observed events were not due to improperly placed cut limits.

(4) Preexisting Δ knockout. Since the struck Δ can only be in the $L \geq 2$ state, the momentum carried by the two remaining nucleons can be appreciable. The $L=2$ signature of the Δ will be smeared by the inelastic interaction with the incident $J=1$ photon, and so three-body ΔNN phase space is assumed for the outgoing momentum distributions. If present, it should contribute much more strongly to the π^+p data set than to the π^-p set.

Figure 5 shows the missing momenta of the π^+p events passing the ‘‘narrow’’ cut, in comparison with these simulations. We see that only the $\Delta^{++}nn$ phase-space model resembles the data; the other simulated mechanisms fail to describe the observed distribution. While direct absorption on three nucleons has been observed previously in photoabsorption studies on ${}^3\text{He}$ [15], a component of the photoabsorption yield with a pure $\Delta^{++}nn$ phase-space distribution has never before been reported. Based on this analysis, we conclude that absorption on a preexisting $\Delta^{++}nn$ configuration in ${}^3\text{He}$ is the best explanation.

The emission angle of the $\pi^\pm p$ system in the frame of the NN recoil ($\theta_{\Delta NN}$) was also reconstructed for every event. Δ^{++} originating from an $L=2$ state should be confined to near $\cos \theta_{\Delta NN} = \pm 1$, while Δ^{++} due to the other processes should be spread more uniformly in this angle. Unfortunately, the effect of the TAGX acceptance and conditions

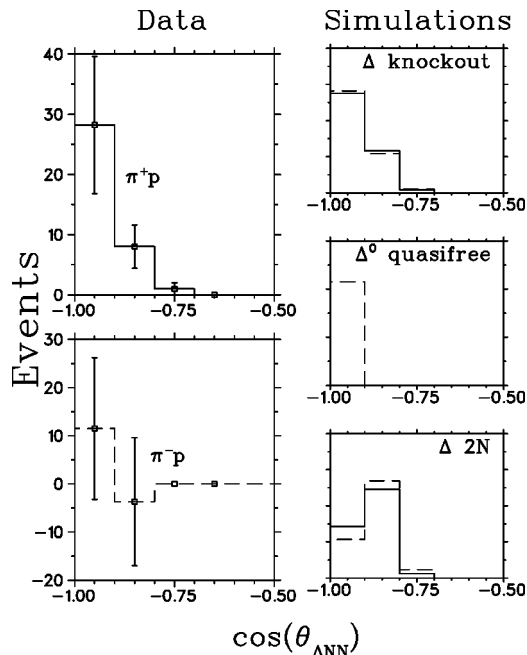


FIG. 6. Reconstructed Δ emission angle in the frame of the recoil NN pair. The left panels show the ${}^3\text{He}(\gamma, \pi^\pm p)$ data obtained with TAGX after application of the cuts described in the text. The line is to guide the eye. The panel on the right shows the expected distribution of events from the various simulated production mechanisms, as labeled. The solid (dashed) lines indicate the π^+p (π^-p) channels, respectively.

TABLE II. Cross sections for the events surviving the stated cuts, assuming a phase-space distribution.

	Narrow cuts	Wide cuts
π^+p	$0.29 \pm 0.08 \mu\text{b}$	$0.39 \pm 0.08 \mu\text{b}$
π^-p	$0.05 \pm 0.07 \mu\text{b}$	$0.10 \pm 0.07 \mu\text{b}$
$\pi^+p : \pi^-p$ ratio	$5.8_{-2.6}$	$3.9_{-0.8}^{+1.7}$
$\pi^+p - \pi^-p$ difference	$0.24 \pm 0.11 \mu\text{b}$	$0.29 \pm 0.11 \mu\text{b}$

(1), (2), and (3) is to restrict all processes to $\cos \theta_{\Delta NN} < 0.7$, but their signatures are still distinctive enough to allow one to distinguish between them. This is shown for the ‘‘narrow’’ cut events in Fig. 6. Only the $\Delta^{++}nn$ phase-space distribution is consistent in shape with the expected signature of Δ knockout, as well as with the data.

The phase-space simulation best describes the observed π^+p and π^-p distributions after application of either the wide or the narrow sets of cuts. Therefore, to obtain the knockout cross section, the appropriately normalized phase-space distribution was integrated over 4π , leading to the cross sections listed in Table II. It should be noted that the acceptances for the two charge states are different, due to the different curvature of the charged particle tracks in the spectrometer’s magnetic field, among other factors. If the observed events are entirely due to Δ^{++} and Δ^0 knockout, the cross sections in Table II should be independent of which sets of cuts are used, and the $\pi^+p : \pi^-p$ ratio should be at least 9:1. As the ratio for the wide cut sample is less than 9:1 by a statistically significant margin, this event sample must not be entirely clean, due to Δ^{++} , Δ^0 photoproduction events and other nonknockout processes which may have survived the cuts. The higher ratio for the narrow cut sample indicates that it is probably much cleaner. A conservative estimate of the lower limit to the Δ^{++} knockout cross section is obtained by taking the difference between the π^+p and π^-p cross sections listed in Table II. This result is reasonably independent of which set of cuts are used, and so the two results are averaged to obtain a Δ^{++} knockout *lower limit* of $0.27 \pm 0.11 \mu\text{b}$.

III. PROBABILITY ESTIMATE

As mentioned earlier, linking the observed Δ^{++} knockout yield to the ΔNN configuration probability requires a model. The actual method used varies tremendously from experiment to experiment. Here, one possibility would be to compare the $\Delta^{++}nn$ absorption probability to the three-body ppn absorption process. However, because the Δ^{++} is initially highly off shell, the inelasticities of the two processes are vastly different, making this comparison nontrivial. We opt to estimate the ΔNN probability in ${}^3\text{He}$ by comparison to the quasifree Δ photoproduction process. In addition to having similar inelasticities, both processes are magnetic dipole transitions, to leading order.

If we assume the ${}^3\text{He}$ wave function to be of the form

$$|{}^3\text{He}\rangle = \sqrt{1 - \beta^2} |ppn\rangle + \beta |\Delta NN\rangle,$$

then the cross section for the Δ^0 quasifree production process is given by

$$|\sqrt{1-\beta^2}\langle\Delta^0 pn|H_{q.f.}|ppn\rangle|^2\frac{dN}{dE^{q.f.}}$$

and that for the Δ^{++} knockout process by

$$|\frac{\beta}{\sqrt{2}}\langle\Delta^{++} nn|H_{k.o.}|\Delta^{++} nn\rangle|^2\frac{dN}{dE^{k.o.}},$$

where dN/dE is the appropriate density of states factor. In the knockout process, the spectator nn pair is in a spin anti-symmetric $L=0$ state, and in the quasifree case the pp are predominantly in this same state, so it is reasonable to expect that the spectators do not contribute to the ratio of the two processes.

Because quasifree Δ^0 production involves a spin flip, it is dominated by the magnetic dipole ($M1$) transition, and Walecka [16] has, using the bag model, related the transition magnetic dipole moment to the nucleon moment,

$$\mu^* = \frac{4}{3\sqrt{2}}\mu_n = 1.8\mu_N,$$

upon substitution of the neutron magnetic moment, $\mu_n = 1.91\mu_N$ [17].

For Δ^{++} knockout, the $E0$ transition is forbidden, since the γ has no charge, and $E1$ is forbidden by parity. Thus, the leading order for this transition should also be $M1$, and the ratio of the matrix elements is, to leading order, proportional to the square of the magnetic dipole moments:

$$\frac{|\langle\Delta^{++}|H_{k.o.}|\Delta^{++}\rangle|^2}{|\langle\Delta^0|H_{q.f.}|n\rangle|^2} = \left(\frac{\mu_{\Delta^{++}}}{\mu^*}\right)^2.$$

We will use the measurement of the Δ^{++} magnetic dipole moment from Ref. [18], $(4.52 \pm 0.50 \pm 0.45)\mu_N$.¹ Including both errors in quadrature leads to a ratio of the squares of the matrix elements, above, of 6.3 ± 1.9 .

If the quasifree Δ^0 cross section is extracted from our data sample, an estimate of β via the above analysis can be made. As the incident photon energy is well above the Δ region, some effort has to be made to isolate the quasifree yield from N^* , multipion, and multinucleon production mechanisms. We apply the same ‘narrow’ condition (2) as before, and now select forward-going Δ 's via the condition

$$|\theta_{\Delta lab}| < 15^\circ \quad (4)$$

and a restrictive missing momentum cut of

¹The Particle Data Group [17] gives their estimate for $\mu_{\Delta^{++}}$ as somewhere between $3.7\mu_N$ and $7.5\mu_N$. However, there is a significant time dependence to the tabulated results, with the older experiments yielding higher values for the magnetic moment than the newer experiments. We believe that Ref. [18] is the most reliable, as it is the most recent measurement.

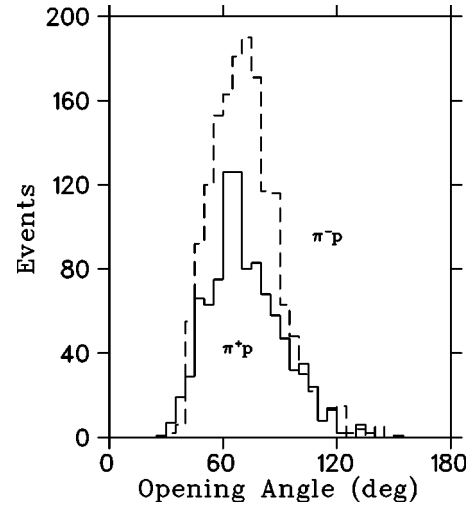


FIG. 7. Laboratory frame opening angle between π and p for data after the application of conditions (2), (4), and (5), as described in the text. An excess of $\pi^- p$ events between opening angle of 40° and 100° is observed, which corresponds to the region accessible to the quasifree process. Outside this range, the $\pi^\pm p$ yields are identical. The excess of $\pi^- p$ over the $\pi^+ p$ yield is assumed to be from quasifree Δ^0 production.

$$\text{missing momentum (PM)} < 185 \text{ MeV}/c \quad (5)$$

serves to isolate the quasifree process.

Figure 7 shows the data remaining after the application of conditions (2), (4), and (5). There is a net excess of $\pi^- p$ events in the region of opening angle appropriate to quasifree Δ^0 photoproduction. Multipion and multinucleon mechanisms should contribute nearly equally to the $\pi^+ p$ and $\pi^- p$ yields, but the quasifree Δ photoproduction mechanism cannot contribute to the $\pi^+ p$ channel. Assuming that all of the excess $\pi^- p$ yield is due to quasifree Δ^0 photoproduction, we obtain a total Δ (charge integrated) photoproduction cross section on ${}^3\text{He}$ of $3.8 \pm 0.4 \mu\text{b}$, after extrapolating to 4π sr. After applying a 20% correction for the difference in the density of states factors for the quasifree and knockout processes (primarily due to the differing three-momenta) and the $M1$ matrix elements, above, we obtain an estimate of $\beta = 0.15$, which corresponds to a lower limit on the ΔNN configuration probability of $1.5 \pm 0.6 \pm 0.5\%$, where the first error listed is statistical, and the second is due to the uncertainty in $\mu_{\Delta^{++}}$. A limitation of this analysis is that it does not take into account off-shell effects due to the deep binding of the ΔNN configuration. This leads to a more compact spatial distribution, reducing the knockout matrix element in a manner not accounted for here, and implying a greater ΔNN configuration probability.

To check this result, the ΔNN probability is independently estimated via an analysis of the missing momentum distribution for the Δ^{++} knockout process. As already mentioned, the ΔNN configuration corresponds to a high momentum component of ${}^3\text{He}$. By assuming that the high momentum tail of the spectral function of Schiavilla, Pandharipande, and Wiringa [14] is due to the ΔNN configuration, we can obtain an upper bound on the probability of

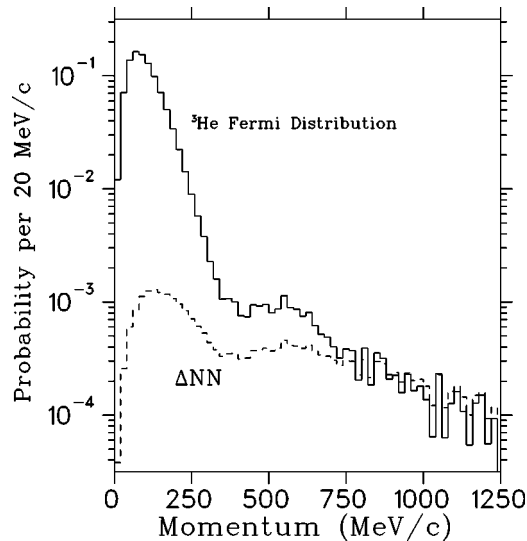


FIG. 8. The solid curve is the unit probability Fermi distribution determined from Ref. [14]. The dashed curve is the probability per unit momentum function for the Δ knockout process, as described in the text.

this configuration. This spectral function is calculated using the Faddeev method, incorporating a realistic treatment of nucleons and Δ 's in nuclear matter. Reference [14] was used to form the ${}^3\text{He}$ Fermi momentum distribution probed by our experiment and normalized to unit probability. The overlap of the ΔNN state with the ${}^3\text{He}$ probability distribution was obtained from the product of the Δ knockout missing momentum distribution and the Fermi distribution, then normalized to the high momentum tail of the unit probability function (Fig. 8). The integral of the probability function gives an estimated upper limit for the ΔNN probability of 2.6%. The uncertainty in this method is limited by the model dependences of the assumed momentum distributions and is difficult to quantify. However, the consistency of the two results is encouraging.

IV. SUMMARY

In conclusion, we have performed an analysis to isolate Δ^{++} knockout from ${}^3\text{He}$ by making use of its unique isospin

and spin properties compared to conventional photoproduction processes. We succeeded in identifying a kinematical region in which a small but statistically significant number of $\pi^+ p$ events were present, with the number of $\pi^- p$ events present in the same region being consistent with zero. This has long been recognized as a strong signal for preexisting Δ 's in ${}^3\text{He}$ [10]. Based on an electromagnetic multipole argument and comparison to the quasifree Δ^0 photoproduction process, we infer a lower limit to the ΔNN probability in ${}^3\text{He}$ of $1.5 \pm 0.6 \pm 0.5\%$. A second method of estimation yielded an upper limit of 2.6%. We believe that the most reliable way to extract the ΔNN configuration probability is to measure the Δ knockout cross section (as done here) and then use a sophisticated nuclear model to calculate the Δ probability corresponding to this cross section. This is the only way that one can be assured that off-shell and Fermi momentum sampling effects have been properly taken into account. We encourage theorists with access to the appropriate tools to take up this challenge.

While the result reported here has a large statistical uncertainty, it should be noted that isolation of ground state Δ components is experimentally very challenging. The consistency of the extracted cross section for different levels of cuts, the good agreement between data and simulations, and the fact that a ΔNN lower limit has been identified all point to an improved Δ probability determination in this work compared to earlier results. Perhaps the sensitivity of electroproduction measurements to the longitudinal Δ knockout process, especially when a transversely polarized target is utilized [19], will allow these experiments to make a more precise statement on the issue of the Δ content of nuclei in the future.

ACKNOWLEDGMENTS

We wish to thank the staff of INS-ES for their considerable help with the experiment and Earle Lomon for his critical reading of the manuscript. This work was supported by grants from the Natural Sciences and Engineering Research Council of Canada (NSERC).

-
- [1] M.R. Anastasio, A. Faessler, H. Muther, K. Holinde, and R. Machleidt, Nucl. Phys. **A322**, 369 (1979).
 [2] E.L. Lomon (private communication). An older version of the model is described in P.G. Blunden, W.R. Greenberg, and E.L. Lomon, Phys. Rev. C **40**, 1541 (1989).
 [3] Additional references for models incorporating nuclear Δ content include: A.M. Green, Rep. Prog. Phys. **39**, 1109 (1976); H.J. Weber and H. Arenhovel, Phys. Rep. **36**, 277 (1978); W. Streuve, Ch. Hajduk, P.U. Sauer, and W. Theis, Nucl. Phys. **A465**, 651 (1987); R. Cenni, F. Conte, and U. Lorenzini, Phys. Rev. C **39**, 1588 (1989); P.G. Blunden, W.R. Greenberg, and E.L. Lomon, *ibid.* **40**, 1541 (1989); A. Picklesimer, R.A. Rice, and R. Brandenburg, *ibid.* **44**, 1359 (1991); M.T. Pena, P.U. Sauer, A. Stadler, and G. Kortemeyer, *ibid.* **48**, 2208 (1993).
 [4] T. Emura *et al.*, Phys. Lett. B **306**, 6 (1993).
 [5] A.I. Amelin *et al.*, Phys. Lett. B **337**, 261 (1994).
 [6] K.I. Blomqvist *et al.*, Phys. Rev. Lett. **77**, 2396 (1996).
 [7] C.L. Morris, J.M. O'Donnell, and J.D. Zumbro, Acta Phys. Pol. B **24**, 1659 (1993); C.L. Morris *et al.*, Phys. Lett. B **419**, 25 (1998).
 [8] E.A. Pasyuk *et al.*, nucl-ex/9912004.
 [9] W. Streuve, Ch. Hajduk, P.U. Sauer, and W. Theis, Nucl. Phys. **A465**, 651 (1987).
 [10] H.J. Lipkin and T.-S.H. Lee, Phys. Lett. B **183**, 22 (1987).
 [11] K. Maruyama *et al.*, Nucl. Instrum. Methods Phys. Res. A **376**, 335 (1996).

- [12] G.J. Lolos *et al.*, Phys. Rev. Lett. **80**, 241 (1998).
- [13] M. Kagarlis *et al.*, Phys. Rev. C **60**, 025203 (1999).
- [14] R. Schiavilla, V.R. Pandharipande, and R.B. Wiringa, Nucl. Phys. **A449**, 219 (1986).
- [15] T. Emura *et al.*, Phys. Rev. Lett. **73**, 404 (1994).
- [16] J.D. Walecka, *Theoretical Nuclear and Subnuclear Physics* (Oxford University Press, Oxford, 1995), Chap. 37.
- [17] Particle Data Group, C. Caso *et al.*, Eur. Phys. J. C **3**, 1 (1998).
- [18] A. Bosshard *et al.*, Phys. Rev. D **44**, 1962 (1991).
- [19] R.G. Milner and T.W. Donnelly, Phys. Rev. C **37**, 870 (1988).